

Fast and Simple Printing of Graded Auxetic Structures

M. A. Carton* and M. Ganter*

*Department of Mechanical Engineering, University of Washington - Seattle, Seattle, WA
98195-2600

Abstract

One of the great promises of additive manufacturing is the ability to build parts with volumetrically graded parameters that would be difficult or impossible with traditional manufacturing. This paper presents a method of procedural generation and unsupported fabrication of 2D objects patterned with functionally graded auxetic (negative Poisson's ratio) cellular structures using commercially available FDM printers. Several types of two-dimensional auxetic pattern are fabricated. The resulting printed objects exhibit a graded response to load, deforming corresponding to local patterning. Deformation is studied using imaging of loaded structures and applications in several areas are considered.

1 Introduction

One advantage of additive manufacturing over conventional manufacturing is the possibility of building in complex internal structure essentially for free. Among the design space that has recently become accessible are functionally graded objects with spatial variation in their material properties (such as stiffness, index of refraction, and electrical conductivity). These properties can be tailored by varying materials or by making a graded internal structure - a varying metamaterial - which causes the structure to have a different material property than its component material or materials. These properties are common among plant and animal structural materials such as wood and spongy bone. A number of graded cellular or lattice structures have been investigated recently, for instance for in applications of energy absorption, piezoelectricity, and small lenses with varying index of refraction. This paper presents a framework for procedural generation of a particular class of printable lattices: graded cellular auxetic parts – that is, materials with a varying negative Poissons ratio.

When expanded in one dimension these materials expand in one or both orthogonal dimensions. Anisotropic auxetic materials can have a Poisson's ratio of well under -1. With rare exceptions [1, 2]) this property is unique to artificial metamaterials. Some of the applications that have been investigated are sensors [3, 4], fasteners [5], textiles [6, 7, 8], protective equipment [9, 3, 10], and medical devices [3]. Auxetics are also being eyed for their property of sinclastic curvature (i.e. positive Gaussian curvature in a sheet upon bending in one direction) which is desirable for the honeycomb composites commonly used in aerospace applications [11, 12, 13, 14].

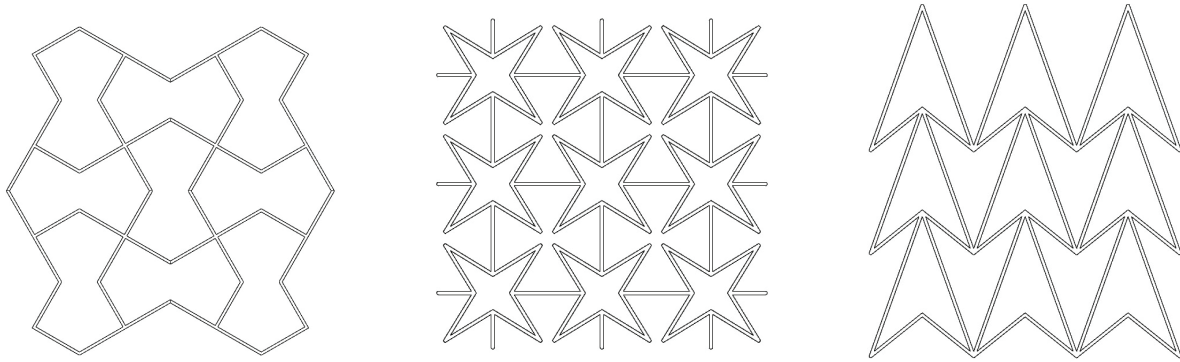


Figure 1: The re-entrant auxetic structures implemented in this project *Left*: Re-entrant octagon (bow structure). *Center*: Re-entrant star. *Right*: Double arrow.

The properties of auxetic materials have been investigated at least since the 19th century [15] but due to their complex internal structures they have been limited in practice until the recent development of computer-aided design and manufacturing. Graded-auxetic and mixed auxetic and non-auxetic materials may be even more valuable. Non-auxetic materials with auxetic inclusions can have a higher Young’s modulus than each material alone [16] and can exhibit auxetic behavior as a whole or even negative thermal expansion [17] and can be designed for unusual load and bending responses [18, 12, 19, 13]. Graded foam structures have shown promising results for improved impact resistance and energy absorption, providing superior response to uniform equivalents under some impact conditions [20, 21, 19]. Parts have been manufactured in a number of ways. Gluing re-entrant and convex cut-fold hexagonal honeycombs produces a sectioned object [22]; finer gradations can be achieved with metal forming and welding [10], and much more easily with additive manufacturing [23, 24].

This paper presents a framework for procedural generation of printable graded auxetic parts. The patterns in figure 1 are generated parametrically, with their geometry determined by a user-defined spatial function. The resulting models, generated in less than two minutes, are simple to design and print.

2 Methods

This section outlines the method used in this code base for procedurally modeling graded cellular structures. Models were generated in Grasshopper, the parametric scripting language of Rhinoceros 3D (RhinoBETA ver. 6.16.19169.14484 for macOS) using the package Clipper to generate curve offsets [25]. This language allows procedural generation of NURBS objects. The code discussed in this section is available at <https://github.com/mollyacarton/auxetic>.

The three patterns chosen for this code are all re-entrant auxetics. Re-entrant cells exhibit auxetic properties when their deformation is dominated by flexure at the joints of the cell [26]. As the cell expands or contracts in one direction, the concave side or sides of the cell open, causing

the cell as a whole to expand or contract. It is easy to show geometrically that altering the internal angle of these types of cellular auxetic patterns alters the resulting Poisson's ratio (for example see the discussion in [11, 27])

Each cell type was modeled as a parametric unit structure. In order to create varying cellular patterns, one of the defining parameters of the shape must be controllable by a user-defined function. In this paper, each of the three patterns chosen has been modeled with a joint in the pattern chosen as the control point. The position of this control point and the points that follow it by symmetry are assigned according to a mapping from the values of the spatial input function. The rest of the shape of the cell is then determined according to this position.

For example, in the star pattern seen in the center of figure 1, the control point is the endpoint of the straight segment connecting each star. Moving this point towards or away from the center of the cell controls the internal angles of the star shape and thus the deformation response of the pattern. When this point is moved away from the center of the cell the internal angles at the points reach perpendicular and the star becomes a square; the pattern is no longer re-entrant and therefore no longer auxetic. As the control point is shifted inward, the internal angle becomes more acute and the theoretical Poisson's ratio increases in the negative direction (top in figure 2). The bow pattern (center in figure 2) similarly consists of octagons with two concave sides, with deformation controlled by the "waist" points of the cell shape. The arrow (sometimes called double arrowhead, bottom in figure 2) is controlled by the point of the arrow.

The code functions as follows. Generate a square grid in the surface-local coordinates (a UV mesh). Then evaluate the spatial function at the center of each cell and map the output to the chosen domain of the controlling parameter. This determines the shape of the individual cell. For some patterns, like the bow and arrow shapes shown in 2 center and bottom, the cells share boundaries. Unlike the star pattern, it is necessary to choose which cell affects which part of the boundary in order to make the boundaries contiguous despite the changing cell shape. In the algorithm, this step is referred to as rectifying boundaries. This is defined by the point that is chosen as a control point; as explained in the previous paragraph, the control points in the bow and arrow patterns both affect the neighboring cells as well as the cell in question. It is possible to classify patterns under "neighbor independent cells" and "neighbor dependent cells" as this affects the localization of response in the pattern.

Once the cells have been generated, the lines are offset by the specified distance and a solid printable part extruded from the 2D pattern. Any additions to the model that are not part of the main cellular pattern, like solid bars for applying load to the flexible part, can be added parametrically or by hand at this step. The parameters to fully define the part depend on the shape, but shared between all the patterns are printing volume parameters such as line width and extrusion depth, as well as grid scale and number of cells in the U and V directions. Treating the structure as a pattern on a UV mesh also provides a basis for mapping to a non-planar surface, although the parts that have been printed so far are planar.



Figure 2: Linear gradation of the three patterns (from top: star, bow, and arrow), open on the left to closed on the right. As the pattern becomes more closed and the internal angles more acute the magnitude of the Poisson's ratio increases.

2.1 Printing

The graded structures shown in figures 3 and 5 were printed on a Creality Ender 3 commercial FFF printer, which has a removable flexible magnetic bed, an advantage for removing well-adhered but delicate structures. The parts in 3 are PLA (polylactic acid) and the part in 5 the more elastic NinjaTek Cheetah TPU (thermoplastic polyurethane) from Fenner Drives, Inc. Prints were sliced in Ultimaker Cura 2.5.0 with a .2 mm layer height. The print temperature was 220°C and the bed temperature of 60°C. TPU was printed at 20 mm/second. Post-processing was limited to removing stray threads of material left by over-extrusion. Each sample part was generated using a 15 mm quadrilateral base cell size.

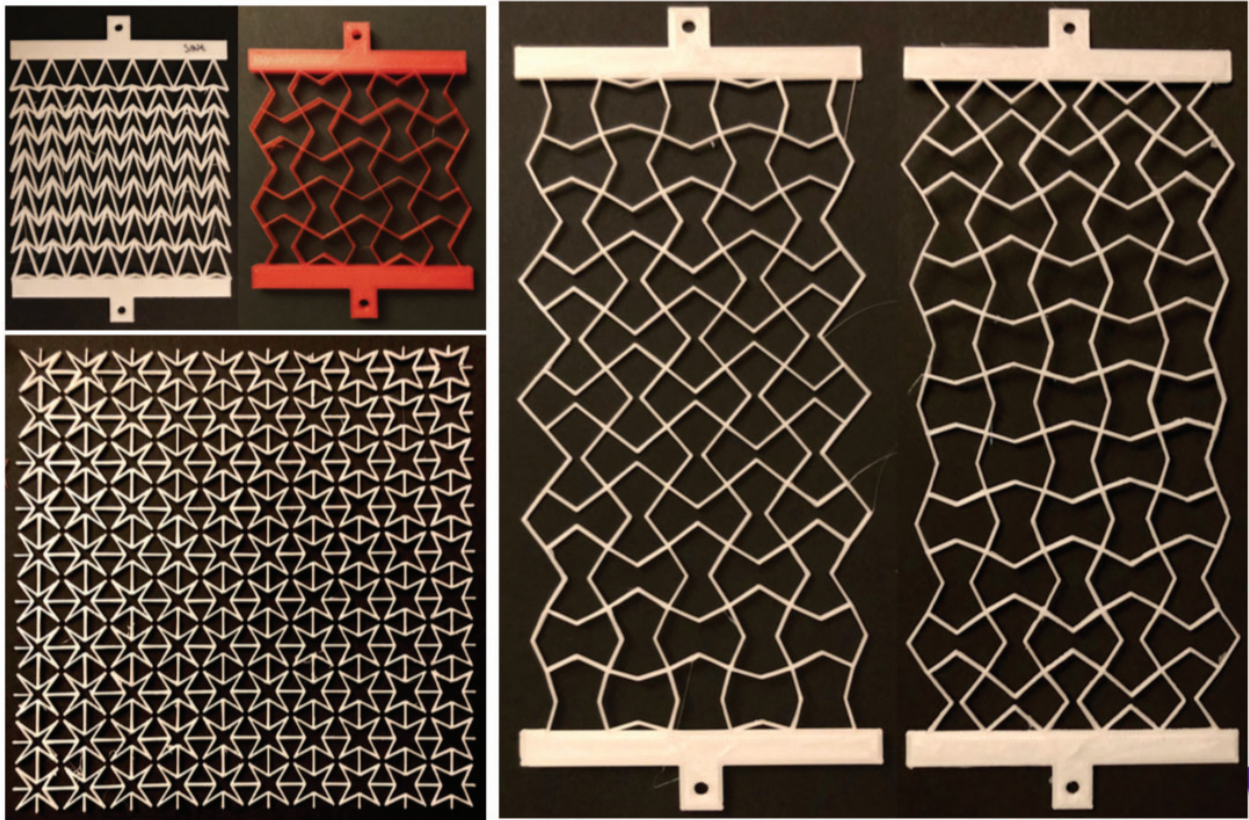


Figure 3: Example printed parts in PLA. The cells are on a square grid with each unit cell 15 mm by 15 mm for all parts.

3 Case Study

The example graded model and its print are shown in figures 4 and 5. This part is a strip of the arrow pattern, 4 by 14 cells, each cell 15 mm. The extrusion height is 5 mm and the line width is .45 mm, corresponding to one print bead width using a .4 mm nozzle. This model was generated in 11.8 seconds. The cells are graded with respect to the function $f(x, y) = |\sin(2\pi y)|$, where the domain in y is $[0, 1]$. This gives a function with two sinusoidal peaks in y . The offset of the control point is between 20% and 80 % of the cell defining scale of 15mm.

The model was simulated in ANSYS Academic ver. 19.2 with a 5 N load applied to the upper edge. The printed part was then equivalently loaded. Image measurements were performed in ImageJ [28], giving an approximate experimental Poisson's ratio $\frac{\Delta x/x_0}{\Delta y/y_0}$ which is plotted in figure 6. This varied between -2.0984 and -0.4426 in an approximately sinusoidal manner.

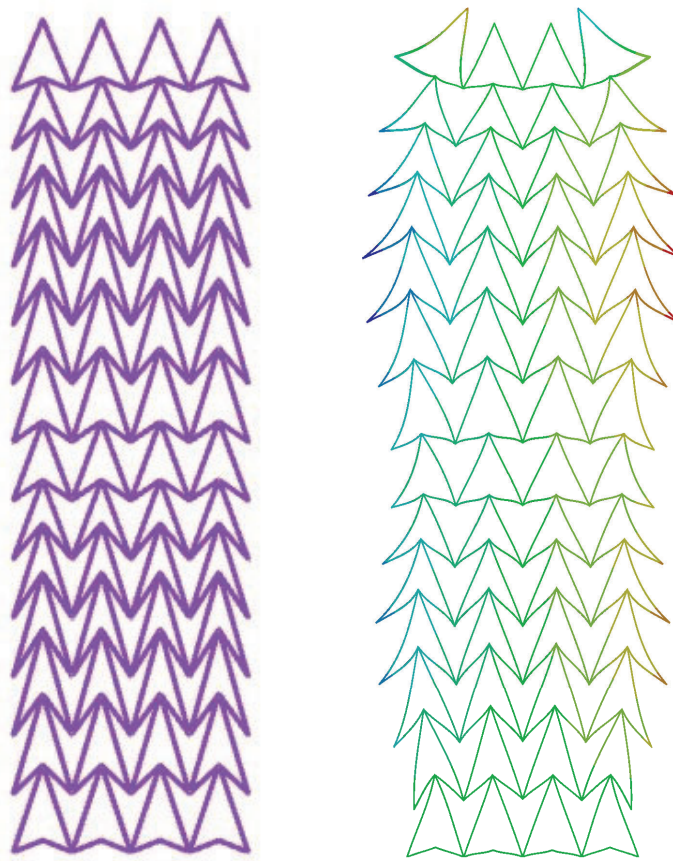


Figure 4: Arrow structure with spatial function $|\sin(2\pi y)|$. *Left:* Original undeformed model. *Right:* Deformation under 5 N load in the y direction applied to the top edge (ANSYS ver. 19.2 Academic). Figures not to scale.

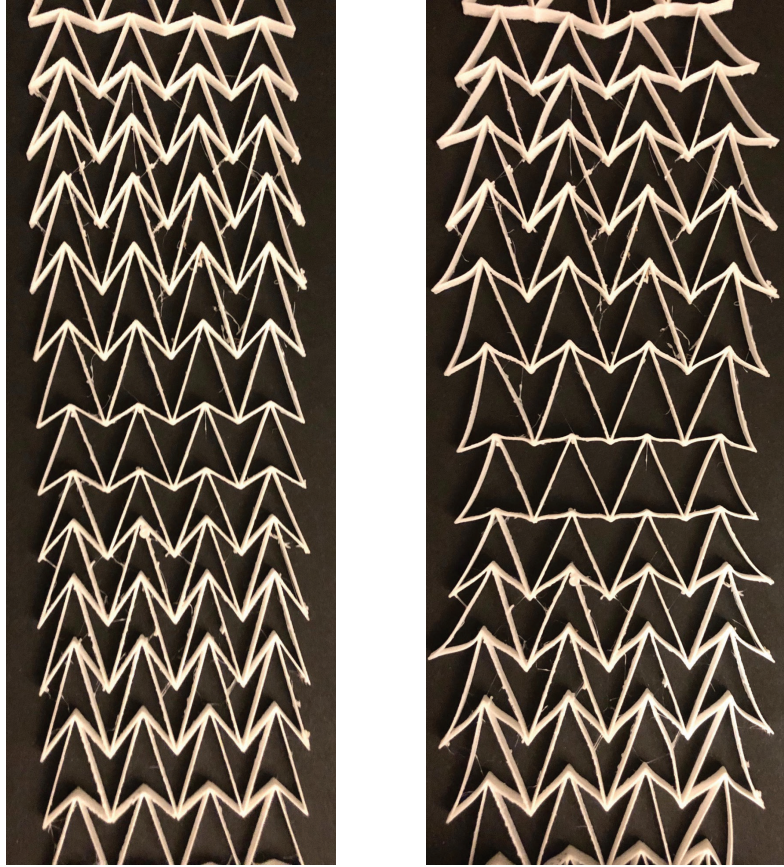


Figure 5: TPU print of the model from figure 4. *Left*: Undeformed *Right*: Deformed.

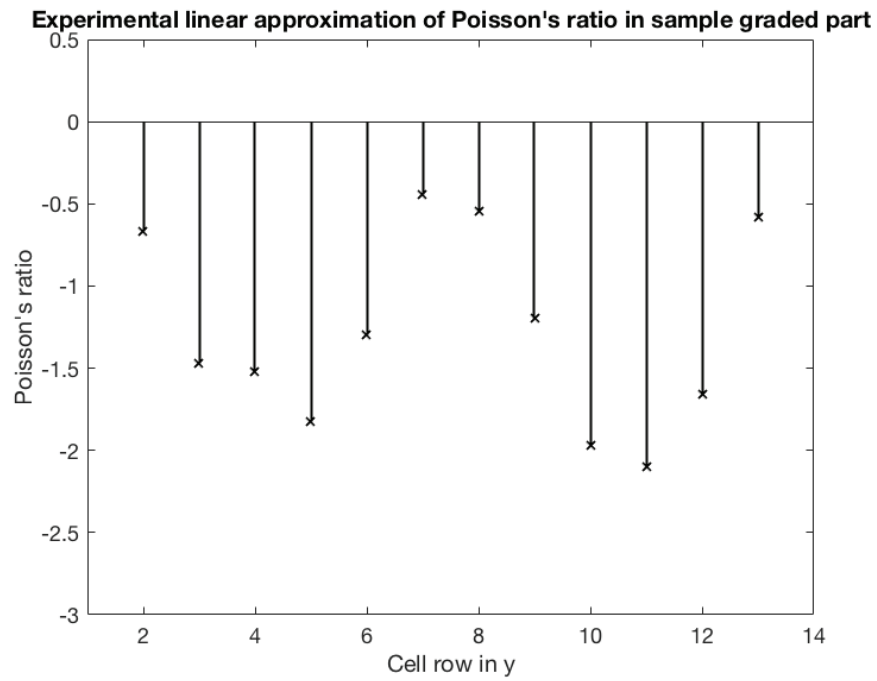


Figure 6: Plot of approximate Poisson's ratio of the TPU printed part shown in figure 5

4 Conclusions

This paper introduced a body of code that generates printable graded auxetic structures through parametric modeling. The code provided in the github repository is available openly for research purposes. An example demonstrates the power of these printed structures - it is possible to print an object that not only has a negative Poisson's ratio but has a varying Poisson's ratio, so that it expands by different amounts in different places. This has possible applications in, for example, fasteners, strain gauges, and piezoelectric devices. A part could be designed that contacts sensors in a specified way when exposed to a certain amount of loading, or causes a secondary activation by physical or electrical contact.

The power of computational design and additive manufacturing is still being uncovered. With more freedom from manufacturing constraints, simple design rules can produce objects with complex behavior, and these resulting objects have only begun to be explored. There is still a need for efficient approaches to procedural generation of lattices and cellular structures, including those with unique material properties like auxetics.

References

- [1] J. Jiang and H. Park, "Negative Poisson's ratio in single-layer black phosphorus," *Nature communications*, vol. 5, p. 4727, 2014.
- [2] A. Marmier, S. Biesheuvel, M. Elmalik, A. Kirke, M. Langhof, J. Paiva, J. Toudup, and K. Evans, "Evidence of negative Poisson's ratio in wood from finite element analysis and off-axis compression experiments," *Materials Letters*, vol. 210, pp. 255–257, 2018.
- [3] Q. Liu, "Literature review: materials with negative Poisson's ratios and potential applications to aerospace and defence," Defence Science and Technology Organisation Victoria (Australia) Air Vehicles Division, Tech. Rep., 2006.
- [4] J. Wong, A. Gong, P. Defnet, L. Meabe, B. Beauchamp, R. Sweet, H. Sardon, C. Cobb, and A. Nelson, "3d printing ionogel auxetic frameworks for stretchable sensors," *Advanced Materials Technologies*, p. 1900452, 2019.
- [5] J. Choi and R. Lakes, "Design of a fastener based on negative Poisson's ratio foam," *Cellular Polymers*, vol. 10, no. 3, pp. 205–212, 1991.
- [6] Z. Wang and H. Hu, "3d auxetic warp-knitted spacer fabrics," *Physica Status Solidi (b)*, vol. 251, no. 2, pp. 281–288, 2014.
- [7] H. Hu and A. Zulifqar, "Auxetic textile materials-a review," *J Textile Engineering Fashion Technology*, vol. 1, no. 1, p. 00002, 2016.
- [8] J. Wright, M. Burns, E. James, M. Sloan, and K. Evans, "On the design and characterisation of low-stiffness auxetic yarns and fabrics," *Textile Research Journal*, vol. 82, no. 7, pp. 645–654, 2012.

- [9] O. Duncan, T. Shepherd, C. Moroney, L. Foster, P. Venkatraman, K. Winwood, T. Allen, and A. Alderson, "Review of auxetic materials for sports applications: Expanding options in comfort and protection," *Applied Sciences*, vol. 8, no. 6, p. 941, 2018.
- [10] Z. Ma, H. Bian, C. Sun, G. Hulbert, K. Bishnoi, and F. Rostam-Abadi, "Functionally-graded npr (negative poisson's ratio) material for a blast-protective deflector," Michigan Univ Ann Arbor, Tech. Rep., 2010.
- [11] F. Scarpa, F. Smith, B. Chambers, and G. Burriesci, "Mechanical and electromagnetic behaviour of auxetic honeycomb structures," *The Aeronautical Journal*, vol. 107, no. 1069, pp. 175–183, 2003.
- [12] Y. Hou, Y. Tai, C. Lira, F. Scarpa, J. Yates, and B. Gu, "The bending and failure of sandwich structures with auxetic gradient cellular cores," *Composites Part A: Applied Science and Manufacturing*, vol. 49, pp. 119–131, 2013.
- [13] C. Li, H.-S. Shen, and H. Wang, "Nonlinear bending of sandwich beams with functionally graded negative poissons ratio honeycomb core," *Composite Structures*, vol. 212, pp. 317–325, 2019.
- [14] Z. Wang, A. Zulifqar, and H. Hu, "Auxetic composites in aerospace engineering," in *Advanced composite materials for aerospace engineering*. Elsevier, 2016, pp. 213–240.
- [15] A. Love, *A treatise on the mathematical theory of elasticity*. Cambridge university press, 1892.
- [16] I. Shufrin, E. Pasternak, and A. Dyskin, "Hybrid materials with negative poissons ratio inclusions," *International Journal of Engineering Science*, vol. 89, pp. 100–120, 2015.
- [17] J. N. Grima, B. Ellul, R. Gatt, and D. Attard, "Negative thermal expansion from disc, cylindrical, and needle shaped inclusions," *Physica status solidi (b)*, vol. 250, no. 10, pp. 2051–2056, 2013.
- [18] T. Lim, "Functionally graded beam for attaining poisson-curving," *Journal of materials science letters*, vol. 21, no. 24, pp. 1899–1901, 2002.
- [19] W. Hou, X. Yang, W. Zhang, and Y. Xia, "Design of energy-dissipating structure with functionally graded auxetic cellular material," *International Journal of Crashworthiness*, vol. 23, no. 4, pp. 366–376, 2018.
- [20] J. Qiao and C. Chen, "Impact resistance of uniform and functionally graded auxetic double arrowhead honeycombs," *International Journal of Impact Engineering*, vol. 83, pp. 47–58, 2015.
- [21] L. Cui, S. Kiernan, and M. Gilchrist, "Designing the energy absorption capacity of functionally graded foam materials," *Materials Science and Engineering: A*, vol. 507, no. 1-2, pp. 215–225, 2009.

- [22] Y. Hou, R. Neville, F. Scarpa, C. Remillat, B. Gu, and M. Ruzzene, “Graded conventional-auxetic kirigami sandwich structures: Flatwise compression and edgewise loading,” *Composites Part B: Engineering*, vol. 59, pp. 33–42, 2014.
- [23] C. Lira, F. Scarpa, and R. Rajasekaran, “A gradient cellular core for aeroengine fan blades based on auxetic configurations,” *Journal of Intelligent Material Systems and Structures*, vol. 22, no. 9, pp. 907–917, 2011.
- [24] E. Khare, S. Temple, I. Tomov, F. Zhang, and S. Smoukov, “Low fatigue dynamic auxetic lattices with 3d printable, multistable, and tuneable unit cells,” *Frontiers in Materials*, vol. 5, p. 45, 2018.
- [25] A. van Waart, “Clipper for grasshopper,” <https://github.com/arendvw/clipper>, Feb 2015.
- [26] K. Evans, A. Alderson, and F. Christian, “Auxetic two-dimensional polymer networks. an example of tailoring geometry for specific mechanical properties,” *Journal of the chemical society, Faraday transactions*, vol. 91, no. 16, pp. 2671–2680, 1995.
- [27] T. Lim, “A 3d auxetic material based on intersecting double arrowheads,” *Physica status solidi (b)*, vol. 253, no. 7, pp. 1252–1260, 2016.
- [28] W. Rasband, “Imagej 1.46r,” <http://imagej.nih.gov/ij>, 2009.